APEM journal
Advances in Production Engineering & Management
Volume 14 | Number 2 | June 2019 | pp 251–263
https://doi.org/10.14743/apem2019.2.326
ISSN 1854-6250
Journal home: apem-journal.org
Original scientific paper

Experimental investigation and multi-objective optimization of micro-wire electrical discharge machining of a titanium alloy using Jaya algorithm

Singh, M.[a], **Ramkumar, J.**[a], **Rao, R.V.**[b,*], **Balic, J.**[c]

[a]Department of Mechanical Engineering, Indian Institute of Technology Kanpur, Kanpur, India
[b]Department of Mechanical Engineering, Sardar Vallabhbhai National Institute of Technology Surat, Surat, India
[c]Faculty of Mechanical Engineering, Laboratory for Intelligent Manufacturing Systems, University of Maribor, Maribor, Slovenia

ABSTRACT

Micro-wire electrical discharge machining (Micro-WEDM) process exhibits superior precision and greater relative accuracy for the efficient machining of difficult-to-machine materials. The micro-slit cutting operation using WEDM process has been experimentally investigated for the objective of analysing the average kerf-loss and responses pertaining to the economic viability of the process viz. average cutting rate and volumetric material removal rate (MRR_v). The experiments are performed using a Tungsten wire of diameter 70 μm on titanium grade 5 alloy (Ti-6Al-4V). Three different controllable process variables (input parameters) associated with the Resistance-Capacitance (RC) based power generator namely discharge energy, wire feed-rate and wire travelling speed are varied to demonstrate their impacts on typical responses such as average kerf-loss, average cutting rate and MRR_v. The experimental analysis revealed a close relationship that cutting rate bears with discharge energy, wire feed-rate and efficient flushing of molten liquid as well as fine debris particles. An advanced multi-objective optimization technique popularly known as Multi Objective-Jaya (MO-Jaya) algorithm has been adopted for the simultaneous optimization of average kerf-loss, average cutting rate and volumetric material removal rate. The best set of input parameters have been selected to suggest the most optimum responses for micro wire-cutting operations.

ARTICLE INFO

Keywords:
Micro-wire electrical discharge machining (Micro-WEDM);
Multi-objective optimization;
Titanium alloy;
Kerf-loss;
Cutting rate;
Volumetric material removal rate;
Feed-rate;
Jaya algorithm;
Multi objective-Jaya algorithm (MO-Jaya)

**Corresponding author:*
ravipudirao@gmail.com
(Rao, R.V.)

Article history:
Received 2 November 2018
Revised 5 May 2019
Accepted 27 May 2019

1. Introduction

Despite several advancements in the applicability of micro-WEDM process, the kerf-loss and its detrimental influence on the relative accuracy and precision have remained an area to be addressed. Due to the occurrence of secondary discharges between the wire and workpiece surface, the feature size is intended to be larger than the wire diameter. Therefore, the width of the feature perpendicular to the motion of wire-travel is commonly termed as kerf-loss. It consists of the diameter of the wire and the radial overcut on either side of the wire. The radial overcut introduces the geometric inaccuracies in the intended feature as it adds the dimension of the feature in addition to the wire diameter. Moreover, the lateral vibration of the wire which is extremely difficult to detect and prevent owing to the complex phenomenon happening in the narrow gap results in the increased kerf-loss [1]. Minimization of kerf-loss demands either reduc-

tion in the diameter of the wire-electrode or lessening in the radial overcut generated during the machining. Owing to the thermal nature of the process there is always a limitation on the minimum diameter of the wire that can be applied productively. Reducing the wire diameter below a certain limit would result in poor tensile strength and consequently ruptures due to thermal softening. Therefore, the reduction of radial/diametric overcut is the only possible way to diminish the kerf-loss. However, a minimum amount of overcutting is always desirable and bound to happen as this narrow pass allows the effective evacuation of fine machining products such as molten liquid and fine debris. Several factors those govern the kerf-loss in the WEDM process include secondary-sparks, bridging of the gap, wire-vibration, low dielectric strength of the fluid, etc. Evacuation of machining products such as fine debris is utmost important for the improved efficiency of the process [2]. Moreover, the electrical and thermal properties of both tool and workpiece material determine the responses in EDM [3] as well as in the WEDM process. However, the non-contact nature of the process makes it a prominent contender for burr-free machining of delicate parts irrespective of its hardness [4]. Fig. 1 shows the schematic diagram of a typical wire slit cutting operation and inclusion of kerf-loss.

Varieties of input parameters affect the material removal rate as well as the kerf-loss in the WEDM process, but the open-circuit voltage and pulse-duration are the noticeable parameters which largely affect the kerf-loss and machining rate [5]. It has also been established that the kerf-loss in the WEDM process is primarily due to the lateral vibration of the wire electrode perhaps caused by the poor wire-tension. Incorporating the appropriate parameters influencing the wire vibration the kerf-loss was reduced with a minimum value of 30.8 μm using a wire of 30 μm diameter [1]. Wire speed has a less significant effect on the outputs as compared to other parameters [5, 6]. The uniformity of sparks across the thickness of the workpiece is essential in minimizing the wire vibration [7]. Majority of the work carried out in the direction of minimization of kerf-loss and maximization of machining rate in the WEDM process is related to the transistor-based circuit where most of the input parameters are arbitrarily decided by the user. However, in the RC based circuit, the capacitance of the capacitor largely determines the discharge-frequency, pulse-duration, pulse-interval and energy per-spark.Therefore, it is essential to establish an experimental analysis pertaining to RC based circuit where the capacitance is the deciding factor. Moreover, the simultaneous optimization of conflicting output responses is paramount importance for the economic viability and improved dimensional accuracy of the process.

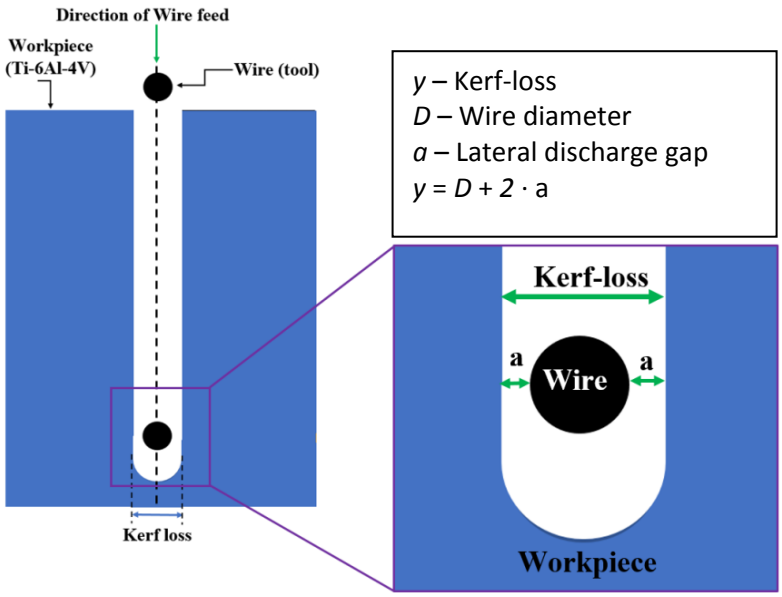

Fig. 1 Schematic illustration of slit cutting operation and the concept of kerf-loss in WEDM process

The rest of the paper is organized into two major sections. The first section consists of the experimentation of micro-slit cutting operation and the influence of various input parameters on the selected output parameters. Finally, adopting an advanced multi-attribute decision-making technique, multi-objective optimization of the micro-WEDM process is conducted, and the results are shown. In order to perform multi-objective optimization of micro-WEDM process, an advanced technique called multi objective-Jaya algorithm is used. The priori approach of the Jaya algorithm first optimizes the individual responses and then convert them into a single objective function to determine the global optimized input parameters and responses.

2. Materials, methods, and design of experiments

The following nomenclature/abbreviations are used in the paper: WEDM: Wire electrical discharge machining; EDM: Electrical discharge machining, MRR_v; Volumetric material removal rate; RC: Resistance capacitance; MO: Multi objective, SEM: Scanning electron microscopic; µm: Micrometer; µJ: Micro Joule; C: Capacitance of the capacitor; V_0: Open circuit voltage; R^2: R square value; Adj. R^2: Adjusted R square value.

The experiments are conducted using the integrated multipurpose machine tool DT-110 (Make Mikrotools Pte. Ltd. Singapore) equipped with an RC based power generator. The micro-WEDM unit available with the machine tool is mounted at the vertical stage of the setup. The micro-WEDM unit consists of a wire-spool, wire guide cum tensioner, wire cutting envelope and a separate spool for collecting the eroded wire. The process parameters which can be varied during the experiments are discharge energy, wire feed-rate and wire travelling speed, whereas the constant parameters consist of charging resistance (1 kOhm), initial spark-gap (20 µm), dielectric fluid (EDM-Oil), wire (Tungsten, 70 µm diameter), wire-tension (15 %). Titanium grade 5 alloy (Ti-6Al-4V) having a thickness of 800 µm has been used as a workpiece material in the study. The discharge energy is a combined term which includes capacitance (C) of the capacitor used and open circuit voltage (V_0) according to the following relationship [8].

$$E = \frac{1}{2} C V_0^2 \tag{1}$$

V_0 is kept constant at 120 V, as the Eq. 1 is pertinent for the condition of maximum energy delivered to the gap [8]. However, the maximum energy condition is hardly fulfilled due to several losses in the process. Therefore, it is the discharge/breakdown voltage which determines the discharge energy. In other cases, the discharge energy is largely influenced by the capacitance value as the discharge voltage invariably remains constant with the constant set of electrodes material, dielectric and inter-electrode-gap.

Exploratory experiments are performed at four distinct levels of discharge energy ranging from 0.72 µJ to 2880 µJ. It has been observed from preliminary experiments that the average cutting rate is exceptionally high at 2880 µJ discharge energy. However, the average kerf-loss and quality of kerf in terms of sharp cutting are observed to be very meagre, and therefore it is recommended to use this energy-level merely for cutting purposes where kerf quality is not a prime interest. The kerf quality of Ti-6Al-4V workpiece machined at two different conditions of discharge energy (2880 µJ and 0.72 µJ) are clearly visualized in Fig. 2(a) and 2(b), respectively. The variation in average cutting rate and average kerf-loss with discharge energy are shown in Fig. 3(a) and 3(b), respectively. A logarithmic scale is used for discharge energy to circumvent the asymmetry of data. It is clearly evident that there is a sudden increase in both average cutting rate as well as average kerf-loss at discharge energy 2880 µJ as compared to other energy levels. Accordingly, the machining operation can be divided into two zones. High energy zone can be used for rough cutting operation whereas the low energy zone is appropriate for the precise cutting operation. Hence, the highest level of discharge energy (2880 µJ) is not considered for detailed experimental investigations. Similarly, the range of feed-rate and wire speed are also determined through preliminary experiments considering the short-circuits and wire-vibration separately.

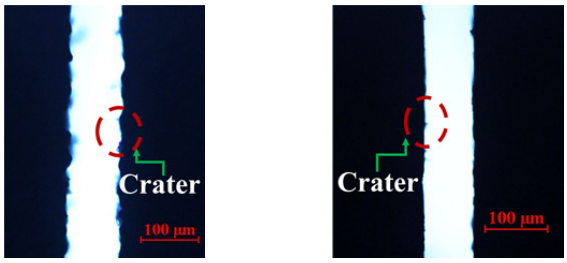

(a) (b)

Fig. 2 Optical microscopic image of slit machined at discharge energy (a) 2880 µJ, (b) 0.72 µJ (Wire feed-rate: 6 µm/s, wire speed: 10 %)

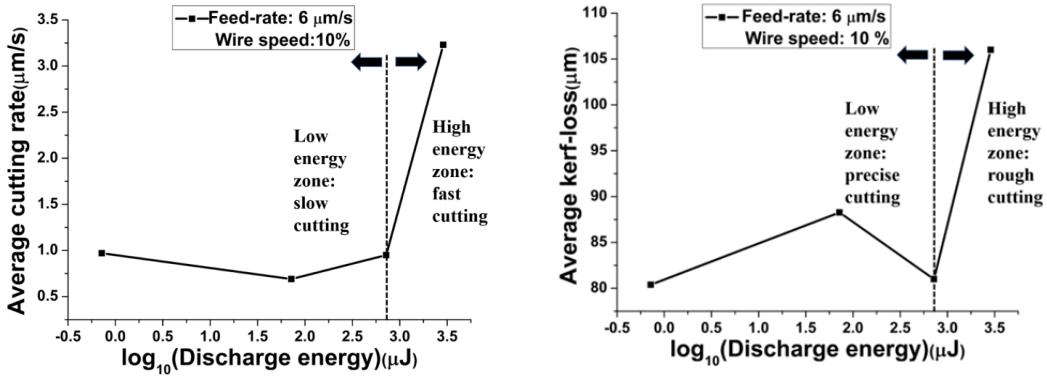

(a) (b)

Fig. 3 Influence of discharge energy on (a) average cutting rate, and (b) average kerf-loss

Table 1 Input parameters and their levels

S. No.	Parameter	Unit	Levels		
1	Discharge energy	µJ	0.72	72	720
2	Feed-rate	µm/s	2	4	6
3	Wire speed	%	10	15	20

Based on the preliminary experiments the ranges of input parameters for detailed experimental investigations are decided. Table 1 displays the three input parameters and their levels used for the slit-cutting operation whereas, Table 2 shows full randomized experimental runs (27) and measured values of responses after conducting the experiments. Std. and Run in Table 2 represent the standard and randomized order of experiments, respectively.

Full factorial design of experiments is performed for analyzing the influence of different process parameters on typical responses. The total number of experiments are $(m)^n = (3)^3 = 27$, where n is the number of factors and m is the number of levels for each factor.

The average kerf-loss is the mean value of the readings of the kerf-width measured at three different locations (inlet, centre and outlet) of the slit. Though the average cutting rate, as well as MRR_v, represent the productivity aspect as well as the rate of machining, yet the MRR_v is related to the total volume of material removed during the operation. Whereas, average cutting rate merely considers the length of the slit machined in the given time and hence neglects the kerf-loss.

$$Average\ cutting\ rate\ (\mu m/s) = \frac{L}{T} \tag{2}$$

where L is the length of the slit machined and T is the total time of machining.

The MRR_v is given as follows [5]:

$$MRR_v\ (\mu m^3/s) = K \cdot t \cdot f \tag{3}$$

where K is the average kerf-loss (µm), t is the thickness of the workpiece (µm), and f is the average cutting rate (µm/s) given by Eq. 2. The workpiece thickness for all experiments is kept constant at 800 µm.

Table: 2 Experimental runs and responses according to full factorial design

Std.	Run	Input parameters			Responses		
		Discharge energy (μJ)	*Feed-rate* (μm/s)	*Wire speed* (%)	*Average kerf-loss* (μm)	*Average cutting rate* (μm/s)	MRR_V $\times 10^3$ ($\mu m^3/s$)
4	1	0.72	4	10	80.35	0.93	59.78
21	2	720	2	20	82.19	0.59	38.79
15	3	720	4	15	80.99	0.71	46
8	4	72	6	10	88.27	0.69	48.73
24	5	720	4	20	83.43	0.56	37.38
13	6	0.72	4	15	79.68	0.89	56.73
17	7	72	6	15	87.93	0.73	51.35
11	8	72	2	15	88.89	0.56	39.82
22	9	0.72	4	20	80.72	0.79	51.02
18	10	720	6	15	80.41	0.81	52.11
12	11	720	2	15	81.17	0.59	38.31
25	12	0.72	6	20	78.99	0.94	59.4
16	13	0.72	6	15	80.74	0.98	63.3
14	14	72	4	15	86.48	0.9	62.27
9	15	720	6	10	79.89	0.95	60.72
3	16	720	2	10	81.20	0.6	38.98
20	17	72	2	20	86.32	0.55	37.98
26	18	72	6	20	87.95	0.93	65.44
2	19	72	2	10	88.13	0.59	41.60
7	20	0.72	6	10	80.38	0.97	62.38
5	21	72	4	10	87.09	0.78	54.35
19	22	0.72	2	20	81.23	0.66	42.89
1	23	0.72	2	10	81.04	0.71	46.03
23	24	72	4	20	88.19	0.83	58.59
27	25	720	6	20	80.92	0.87	56.32
6	26	720	4	10	80.30	0.86	55.25
10	27	0.72	2	15	80.72	0.72	46.50

3. Results and discussion

The typical responses of interest include average cutting rate, MRR_V and average kerf-loss. The responses are analyzed with the variation in input-parameters used in the study.

3.1. Effect of discharge energy

Fig. 4(a) shows the variation in average cutting rate with discharge energy. It is clearly evident from the graph that the average cutting rate is invariably constant at lowest (0.72 μJ) and highest (720 μJ) discharge energy levels used in the study. Though there is a considerable increase in the discharge energy, the feed-rate and flushing conditions are such that the substantial improvement in machining rate is not achieved. It can be attributed to the fact that an increase in discharge energy increases the volume of material removal per-spark, so the quantity of molten material which is to be removed is large. However, the feed-rate, as well as flushing conditions, are not adequate to remove the whole liquid metal and therefore the expected increase in machining rate is not achieved. The combination of sparks frequency and discharge energy suggest that at lower discharge energy the sparks frequency is high, but the volume of material per pulse is small. Whereas at the high discharge energy level the volume of molten material per pulse is large but low sparks frequency allows adequate pulse-off duration for the evacuation of molten material pool and debris. However, at the intermediate value of discharge energy, the combination of sparks frequency and molten volume of material is critical to remove it efficiently. This can be established by the fact that the average cutting rate at 72 μJ is lower than that at 0.72 μJ. The inability to remove the entire molten material in the frontal gap prevents the wire to proceed forward and therefore more interaction time is available for secondary discharges to happen. This fact can be clearly verified by the increased kerf-loss at this energy level as shown in Fig. 4(c). The same phenomenon is responsible for MRR_v though it is slightly higher owing to larger kerf-loss at 72 μJ, Fig. 4(b). Therefore flushing is an utmost important factor to consider in the micro-EDM as well as micro-WEDM process [9]. Moreover, an exact trend is difficult to es-

tablish in RC based power generator due to variation in charging of capacitor [10].The average kerf-loss at the lowest and highest energy levels are not considerably different. The constant value of feed-rate enables the servo system to move with constant speed and, therefore, the time available for secondary sparks to occur is invariably the same. Though the volume of the crater formed with higher discharge energy is large yet the frequency of sparks is low as the higher discharge energy is achievable with increased capacitance value. Higher the value of capacitance greater will be the discharge energy and lower is the frequency of sparks.

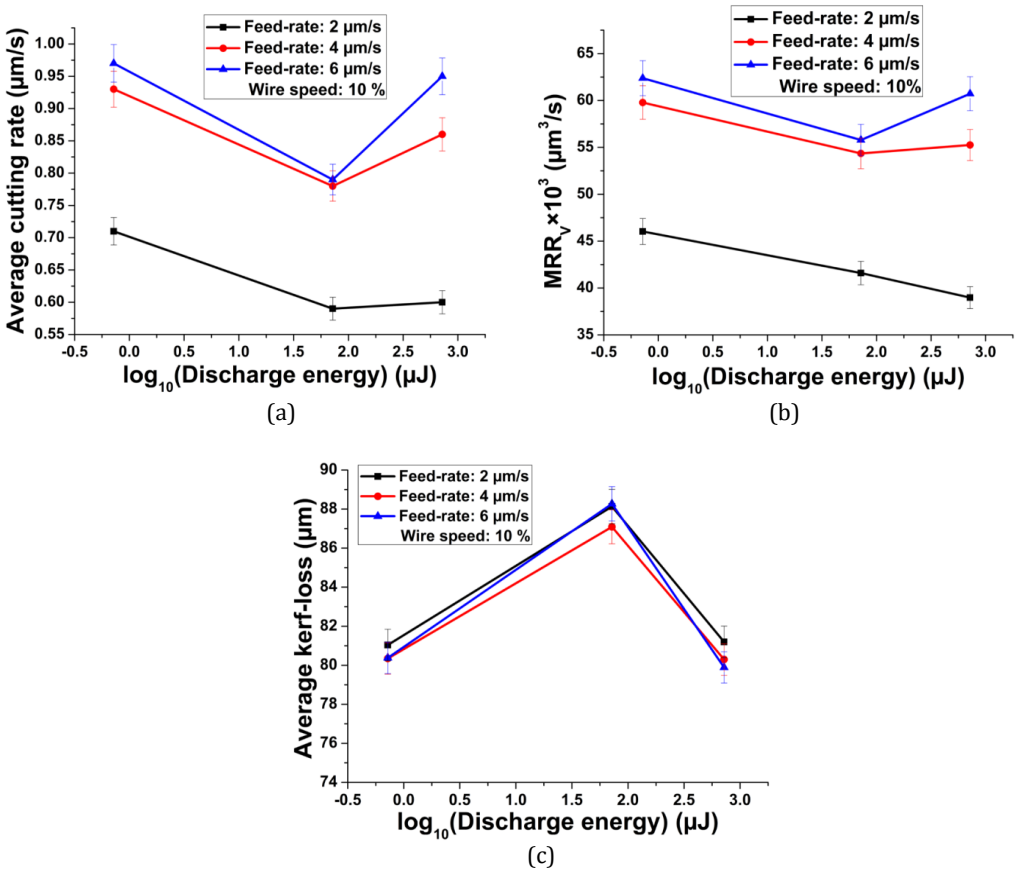

Fig. 4 Influence of discharge energy on: (a) average cutting rate, (b) MRR_v and (c) average kerf-loss

3.2 Effect of wire feed-rate

The average cutting rate increases continuously with an increase in wire feed-rate in the given range. Wire feed-rate in the micro-WEDM/EDM process comes into action only when there is a short circuit between wire and workpiece or there is a gap enlargement due to the formation of the crater. In both the situations, the wire is either retracted away from the workpiece or moves forward to maintain an equilibrium gap with speed specified by the user termed as wire feed-rate. Therefore, the non-productive time associated with wire retraction in case of short circuit and forward motion to adjust the gap reduces with the increased wire feed-rate. Both the average cutting rate as well as MRR_v increases with the increase in wire feed-rate in the given range of 2-6 µm/s, Fig. 5(a) and 5(b). However, beyond a certain value further increase in wire feed-rate, continuous short circuits are observed and machining ceases. Therefore, the judicious decision must be taken while selecting the appropriate wire feed-rate. However, the preliminary experiments have revealed the use of wire feed-rate as high as 10-15 µm/s with discharge energy of 2880 µJ as the large volume of molten material creates a large size crater.

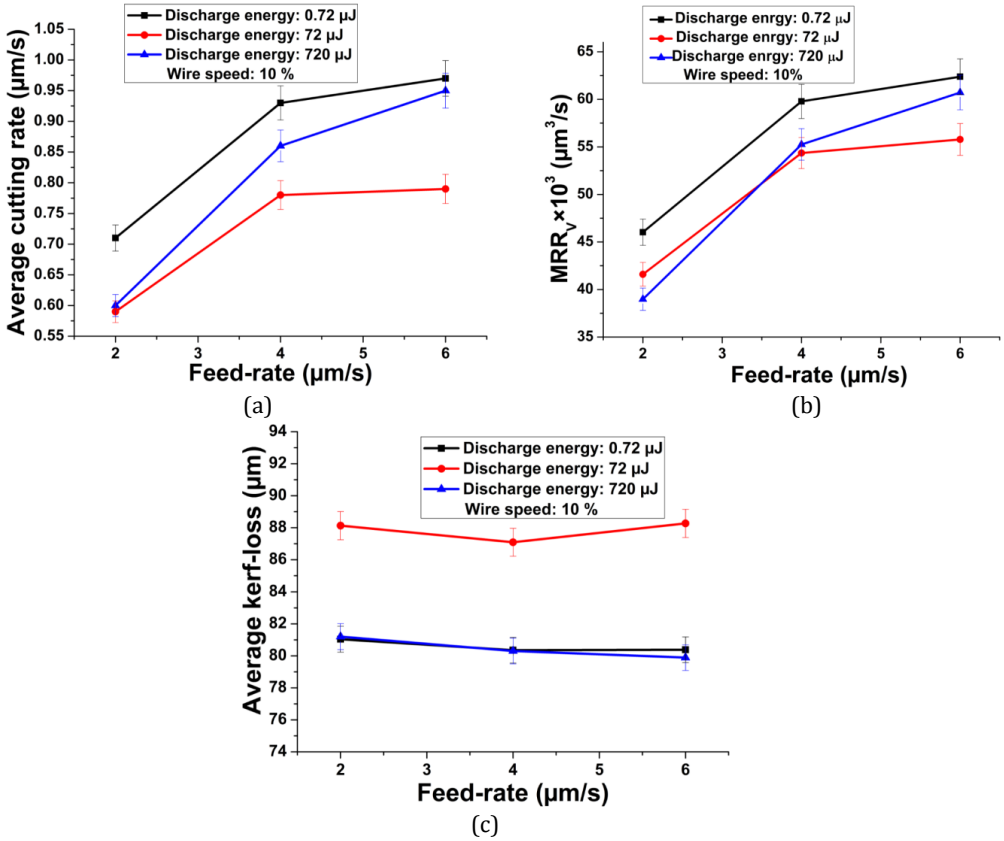

Fig. 5 Influence of wire feed-rate on (a) average cutting rate, (b) MRR_v and (c) average kerf-loss

The average kerf-loss is not much influenced by the wire feed-rate though it is decreasing slightly at 720 µJ and 0.72 µJ discharge energy levels. The occurrence of secondary sparks decreases as the wire travels with higher feed-rate and thus the kerf-loss reduces slightly. At 72 µJ discharge energy the average kerf-loss is observed to be decreasing with an increase in wire feed-rate from 2 µm/s to 4 µm/s and then it increases slightly at 6 µm/s, Fig. 5(c), due to frequent short circuits as the wire is not able to move forward and more secondary sparks are taking place in the lateral gap.

3.3 Effect of wire travelling speed

The wire travelling speed refers to the speed of wire circulation from the wire supplying wheel to the wire collecting wheel. The prevalent phenomenon of tool wear in EDM as well as WEDM process necessitates the wire to travel continuously so that a fresh or uneroded wire can be presented for cutting operation. If the wire is stationary, then the high temperature in the vicinity of the plasma channel would reduce its tensile strength and eventually the wire breaks. However, higher wire travelling speed results in the consumption of more wire. Therefore, the wire speed is decided while considering the wire breakage and less consumption simultaneously. The Fig. 6(a) and 6(b) reveal a less significant influence of wire speed on both average cutting rate and MRR_v. This insignificant variation of output parameters with wire speed is also supported by the study conducted in [5]. A slight decrease in the responses with an increase in wire speed from 15-20 % is attributed to the vibration of wire resulting from the vibration induced in the wire guides as the speed increases. The average kerf-loss is not considerably affected by the wire speed as the number of secondary sparks are not reduced significantly with the variation in wire speed. However, at 72 µJ discharge energy, it is observed that the increased wire speed improves the flushing of molten material in the frontal gap and therefore the interaction of the wire in the lateral gap reduces. This can be established with a decrease in kerf-loss at 72 µJ discharge energy while increasing the wire speed from 15-20 %, Fig. 6(c).

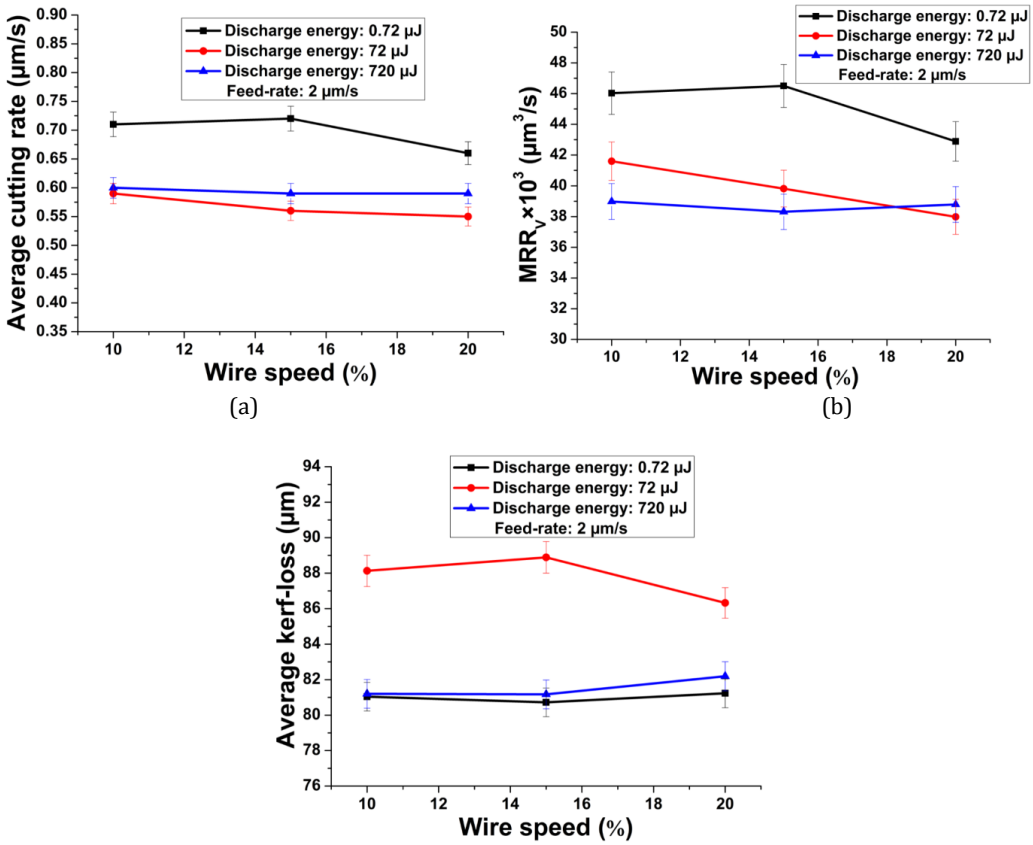

Fig. 6 Influence of wire speed on (a) average cutting rate, (b) MRR_v and (c) average kerf-loss

3.4 Multi-objective optimization of the micro-WEDM process with multi objective-Jaya (MO-Jaya) algorithm

Multi-objective optimization problem deals with the assertion of the best set of input parameters in the given range to satisfy the responses with conflicting desirability simultaneously [11]. The values of process parameters used in experimental investigations are rarely optimum, and thus multi-objective optimization is required to come with the optimum set of input parameters [12]. The micro slit-cutting operation presented in current work consists of three responses with contradictory natures, i.e. two of them (average cutting rate and MRR_v) demand maximization whereas one of the responses (average kerf-loss) is to be minimized. The problem of synchronized optimization of various responses with incompatible desirability is categorized as a multi-objective optimization problem.

Multi objective-Jaya (MO-Jaya) algorithm

Jaya algorithm is an advanced optimization technique. Unlike other similar techniques such as genetic algorithm, particle swarm algorithm and artificial bee colony algorithm, the Jaya algorithm doesn't have algorithm specific parameters which sometimes affect the final results if a fine tuning between the parameters specific to the algorithm is not achieved [13-14].

The multi-objective optimization consists of the determination of global optimum input parameters which can simultaneously satisfy all the conflicting responses. The optimum values of each response while solving them individually are used to convert them into a single/combined objective function. The single objective function is either maximized or minimized to evaluate the optimum global values of input parameters. This method is termed as a priori approach of the Jaya algorithm.

The present experimental analysis of micro-WEDM process consists of three input parameters and three number of output responses which are expressed in the mathematical form in Eqs. 4, 5 and 6. The prediction models given by Eqs. 4, 5 and 6 represent the output responses

such as average cutting rate, MRR_v and average kerf-loss respectively in terms of input parameters. These prediction models can predict the output at distinct levels of input parameters in the given range. Among three output responses, average kerf-loss is to be minimized whereas the other two namely average cutting rate and MRR_v are to be maximized. Performing regression analysis, the quadratic prediction models for each response in terms of input parameters are obtained as follows.

Average cutting rate:

$$f_1 = 0.520896284 - 0.001555172 \cdot A + 0.149297749 \cdot B - 0.00829 \cdot C + 2.22741 \cdot 10^{-6} \cdot A^2 - 0.014722222 \cdot B^2 + 4.44444 \cdot 10^{-5} \cdot C^2 + 1.36956 \cdot 10^{-5} \cdot A \cdot B + 0.001916667 \cdot B \cdot C - 1.781 \times 10^{-5} \cdot C \cdot A \quad (4)$$

Volumetric material removal rate:

$$f_2 = 33734.23458 - 34.2746937 \cdot A + 9953.068531 \cdot B - 684.5006238 \cdot C + 0.051817546 \cdot A^2 - 1001.25 \cdot B^2 + 6.333333333 \cdot C^2 + 0.592846241 \cdot A \cdot B + 135.6666667 \cdot B \cdot C - 1.023688223 \cdot C \cdot A \quad (5)$$

Average kerf-loss:

$$f_3 = 82.82242011 + 0.109846399 \cdot A - 0.291825702 \cdot B - 0.210612268 \cdot C - 0.000155738 \cdot A^2 + 0.026527778 \cdot B^2 + 0.005711111 \cdot C^2 - 0.00024381 \cdot A \cdot B - 0.000416667 \cdot B \cdot C + 0.000293298 \cdot C \cdot A \quad (6)$$

where A, B and C are the actual values of discharge energy (μJ), wire feed-rate (μm/s) and wire speed (%), respectively. The accuracy of the quadratic fit models is adjudged by the values of R^2 and adj. R^2 for each case. The R^2 and adj. R^2 values are 0.78 and 0.66 for f_1, 0.76 and 0.64 for f_2 and 0.96 and 0.94 for f_3.

The flowchart (Fig. 7) shows the various steps involved in the Jaya algorithm. The same steps are executed for individual optimization of each output response and multi-objective optimization when a combined objective function is used.

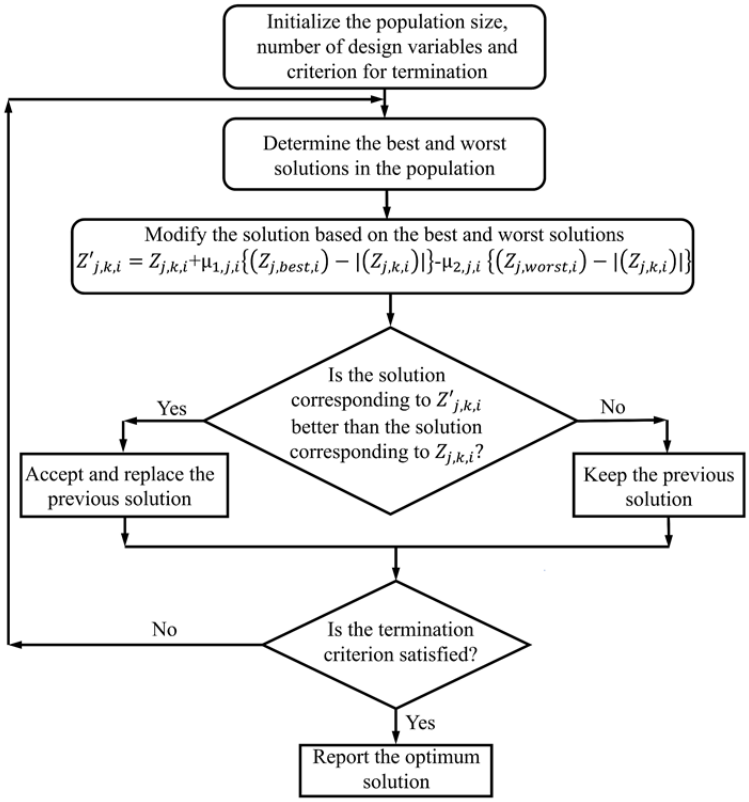

Fig. 7 Flowchart showing the steps in the Jaya algorithm

Individual optimization

First of all, the three output responses given by the regression Eqs. 4, 5 and 6 are optimized separately without taking into consideration the other two outputs. For this step, the regression equation of the respective output responses is assumed to be an objective function.

- (i)The input variables pertaining to Jaya algorithm such as the number of design variables (equal to the number of input parameters, i.e. three), population size (number of candidate solutions) and the termination criterion (i.e. the number of iterations) are decided by the decision maker.
- (ii)The design variables, i.e. the input parameters are assigned the random values in the given range of the respective variables. The range for different variables is: A (0.72-720 μJ), B (2-6 μm/s), C (10-20 %).
- (iii)For each candidate solution, the value of the objective function is calculated. The best and worst value of the objective function is determined. For a maximization problem, the best value corresponds to the maximum value of objective function across all the candidate solutions whereas the worst value corresponds to the minimum value of the objective function. The vice-versa is true for a minimization problem. The corresponding values of input parameters are known as the best and worst values for the respective input parameter.
- (iv)The values of the design variables for each candidate solution is modified as per the following equation [15]:

$$Z'_{j,k,i} = Z_{j,k,i} + \mu_{1,j,i}\left\{\left(Z_{j,\,best,i}\right) - \left|\left(Z_{j,k,i}\right)\right|\right\} - \mu_{2,j,i}\left\{\left(Z_{j,worst,i}\right) - \left|\left(Z_{j,k,i}\right)\right|\right\} \quad (7)$$

  where, $Z'_{j,k,i}$ is the new value of $Z_{j,k,i}$, $Z_{j,\,best,i}$ and $Z_{j,worst,i}$ are the value of objective function corresponding to the best candidate and worst candidate respectively. $\mu_{1,j,i}$ and $\mu_{2,j,i}$ are two random numbers between 0 and 1.
- (v) Step (iii) is repeated.
- (vi) Compare the values of the objective functions of different candidate solutions in step (v) with the corresponding values of step (iii). If the value of the objective function in step (v) is better than that in step (iii), this new value is accepted along with the corresponding input parameters. Else, the previous solution is retained.
- (vii) This completes one iteration. The algorithm continues to execute until the last iteration at which the values of all candidate solutions become equal.

The value of the objective function and input parameters are accepted as the optimum value of output and input parameters respectively. A similar procedure is repeated for the other two output responses. The optimum values of output responses and the corresponding optimum input parameters while solving them distinctly are given in Table 3. Max_f_1, Max_f_2 are the optimum values of outputs f_1 and f_2, respectively, while solving them individually for maximization whereas Min_f_3 is the optimum value of f_3 while solving it for minimization using Jaya algorithm.

Table 3 Optimized results obtained by using Jaya algorithm when each response is solved individually

Responses	The optimum value of the response	Optimum discharge energy (μJ): A	Optimum feed-rate (μm/s): B	Optimum wire speed (%): C
Max_f_1 (μm/s)	1.2990	0.72	6	20
$Max\_f_2 \times 10^3$ (μm³/s)	62.4941	0.72	6	20
Min_f_3 (μm)	78.1048	720	6	10

Multi-objective optimization

The optimum input parameters given in Table 3 are pertinent only when one of the outputs is to be looked-for while neglecting the other two. However, the success of any process is determined by the combined effects of all output parameters. Therefore, the multi-objective optimization is performed to come up with a set of best input parameters that can satisfy all the responses sim-

ultaneously. This can be achieved by converting the outputs with conflicting desirability into a single objective function and then optimizing that combined objective function.

In the present study the combined objective function is formulated by the following equation:

$$Z_{Max} = \frac{f_1}{Max\_f_1} + \frac{f_2}{Max\_f_2} - \frac{f_3}{Min\_f_3} \tag{7}$$

Here, f_1, f_2, f_3 are the prediction models given by Eqs. 4, 5 and 6, respectively, whereas Max_f_1, Max_f_2, Min_f_3 are the optimized values of f_1, f_2 *and* f_3 given in Table 3. Negative sign in the third term indicates the conversion of minimization problem (Min_f_3) into a maximization problem (Z_{Max}).

The Jaya algorithm is repeated while considering Z_{Max} to be the objective function. The Jaya algorithm used for this optimization is named as multi objective-Jaya algorithm. The algorithm is executed using a rigorous MATLAB code written in version R2016a (9.0).

The global optimum input parameters satisfying all the output responses simultaneously are given in Table 4. Putting these optimum input values into the regression Eqs. 4, 5 and 6, the corresponding optimum values of responses are also calculated.

MO-Jaya algorithm predicts minimum value of discharge energy (0.72 μJ) and maximum values of feed-rate (6 μm/s) and wire speed (20 %) as an optimum input parameters for simultaneous optimization of three output response. The global optimum input parameters correspond to experiment number 12 of Table 2. Fig. 8(a) shows the optical microscopic image of the micro-slit machined at the global optimum input parameters. Whereas Fig. 8(b) shows the SEM image of a micro-slit machined. The magnified view of the machined surface reveals the formation of recast layer due to the re-solidification of molten liquid. Therefore, the appropriate flushing of molten liquid and debris particles is a paramount necessity for superior dimensional accuracy as well as the better surface characteristics of the process. Fig. 8(c) depicts the uniformity of slit width along the workpiece length and thickness respectively.

Table 4 Results of MO-Jaya algorithm for multi-objective optimization

	Global optimum input parameters			Corresponding optimum values of responses		
Parameters	*Discharge energy* (μJ): A	*Feed-rate* (μm/s): B	*Wire speed* (%): C	*Kerf-loss* (μm)	*Average cutting rate* (μm/s)	$MRR_v \times 10^3$ (μm³/s)
Values	0.72	6	20	80.1790	1.2990	62.4941

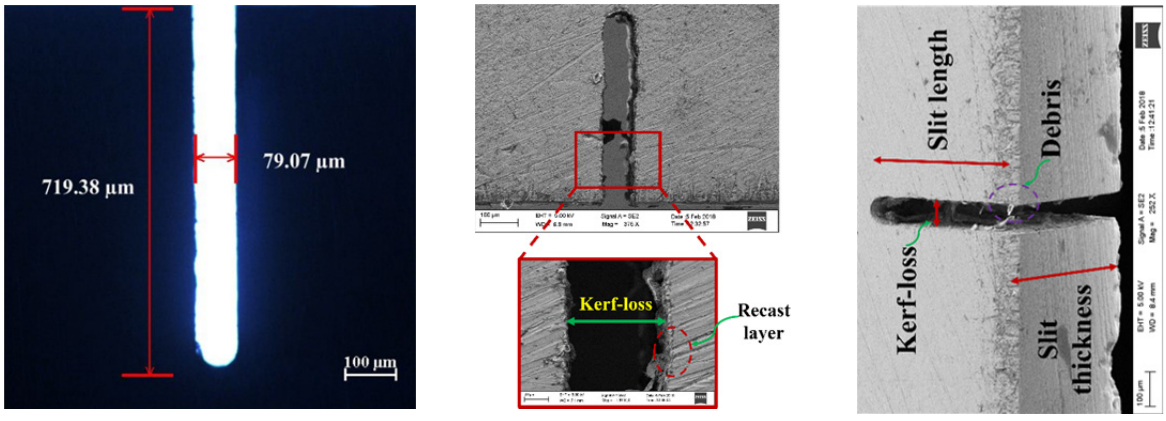

(a) (b) (c)

Fig. 8 (a) Optical microscopic image of optimized slit according to MO-Jaya method (Experiment No. 12, Table 2) (b) SEM image of a slit machined (c) SEM image of a slit machined showing kerf-loss along the length and thickness (720 μJ discharge energy and 6 μm/s feed-rate)

4. Conclusions

The paper discusses the variation in average cutting rate, MRR_v and average kerf-loss with input parameters such as discharge energy, wire feed-rate and wire speed. Further, an exertion has been made to obtain the global optimum parameters for simultaneous optimization of various conflicting responses. Following conclusions have been drawn from the work presented in the paper:

- On the basis of preliminary experiments for average cutting rate and average kerf-loss, it is observed that for rough cutting operation where the kerf quality is not utmost important the highest energy level (2880 μJ) can be used. However, for the precise cutting operation, it is recommended to use lower discharge energy levels (0.72-720 μJ).
- Unlike theoretical prediction, the average cutting rate and MRR_v have a close relation with discharge energy, wire feed-rate and efficient flushing of molten material as well as debris particles. The adequate flushing condition is essential for the requisite improvement in machining rate.
- A maximum average cutting rate of 0.98 μm/s and MRR_v of 65.44 $\times 10^3$ $\mu m^3/s$ are reported from the experimental investigations. Whereas the minimum value of average kerf-loss using a tungsten wire (70 μm diameter) is found to be 78.99 μm which implies that the diametral overcut is 12.84 % of the wire diameter. Therefore, the minimum radial side gap of 4.49 μm on either side of the wire is attained.
- Multi objective-Jaya algorithm has been applied for the simultaneous optimization of output responses. The algorithm results suggest minimum discharge energy (0.72 μJ), highest wire feed-rate (6 μm/s) and wire speed (20 %) as the global optimum input parameters.
- Unlike the other advanced optimization algorithms, the MO-Jaya algorithm doesn't have algorithm-specific parameters and this is an advantageous feature. The presence of algorithm-specific parameters in other optimization algorithms may adversely affect the final results if a fine tuning between the algorithm-specific parameters is not achieved. However, the proposed MO-Jaya algorithm needs to be run many times so as to get a Pareto front to get non-dominated solutions if different weights are to be assigned to the objectives.
- Multi-objective optimization with some other advanced evolutionary computation and swarm intelligence optimization methods will be taken up in near future.
- The future prospects of the micro-WEDM process would include thin wall micromachining of Ti-6Al-4V.

References

[1] Di, S., Chu, X., Wei, D., Wang, Z., Chi, G., Liu, Y. (2009). Analysis of kerf width in micro-WEDM, *International Journal of Machine Tools and Manufacture,* Vol. 49, No. 10, 788-792, doi: 10.1016/j.ijmachtools.2009.04.006.

[2] Narasimhan, J., Yu, Z., Rajurkar, K.P. (2005). Tool wear compensation and path generation in micro and macro EDM, *Journal of Manufacturing Processes,* Vol. 7, No. 1, 75-82, doi: 10.1016/S1526-6125(05)70084-0.

[3] D'Urso, G., Ravasio, C. (2017). Material-technology index to evaluate micro-EDM drilling process, *Journal of Manufacturing Processes,* Vol. 26, 13-21, doi: 10.1016/j.jmapro.2017.01.003.

[4] Joshi, S.N., Pande, S.S. (2010). Thermo-physical modeling of die-sinking EDM process, *Journal of Manufacturing Processes,* Vol. 12, No. 1, 45-56, doi: 10.1016/j.jmapro.2010.02.001.

[5] Tosun, N., Cogun, C., Tosun, G. (2004). A study on kerf and material removal rate in wire electrical discharge machining based on Taguchi method, *Journal of Materials Processing Technology,* Vol. 152, No. 3, 316-322, doi: 10.1016/j.jmatprotec.2004.04.373.

[6] Scott, D., Boyina, S., Rajurkar, K.P. (1991). Analysis and optimization of parameter combinations in wire electrical discharge machining, *International Journal of Production Research,* Vol. 29, No. 11, 2189-2207, doi: 10.1080/00207549108948078.

[7] Okada, A., Uno, Y., Nakazawa, M., Yamauchi, T. (2010). Evaluations of spark distribution and wire vibration in wire EDM by high-speed observation, *CIRP Annals,* Vol. 59, No. 1, 231-234, doi: 10.1016/j.cirp.2010.03.073.

[8] Masuzawa, T., Tönshoff, H.K. (1997). Three-dimensional micromachining by machine tools, *CIRP Annals,* Vol. 46, No. 2, 621-628, doi: 10.1016/S0007-8506(07)60882-8.

[9] Karthikeyan, G., Ramkumar, J., Dhamodaran, S., Aravindan, S. (2010). Micro electric discharge milling process performance: An experimental investigation, *International Journal of Machine Tools and Manufacture,* Vol. 50, No. 8, 718-727, doi: 10.1016/j.ijmachtools.2010.04.007.

[10] Jahan, M.P., Wong, Y.S., Rahman, M. (2009). A study on the quality micro-hole machining of tungsten carbide by micro-EDM process using transistor and RC-type pulse generator, *Journal of Materials Processing Technology,* Vol. 209, No. 4, 1706-1716, doi: 10.1016/j.jmatprotec.2008.04.029.
[11] Konak, A., Coit, D.W., Smith, A.E. (2006). Multi-objective optimization using genetic algorithms: A tutorial, *Reliability Engineering & System Safety,* Vol. 91, No. 9, 992-1007, doi: 10.1016/j.ress.2005.11.018.
[12] Rao, R.V., Rai, D.P., Balic, J. (2017). A multi-objective algorithm for optimization of modern machining processes, *Engineering Applications of Artificial Intelligence,* Vol. 61, 103-125, doi: 10.1016/j.engappai.2017.03.001.
[13] Rao, R.V. (2019). *Jaya: An advanced optimization algorithm and its engineering applications,* Springer International Publishing AG, Cham, Switzerland, doi: 10.1007/978-3-319-78922-4.
[14] Rao, R.V., Rai, D.P., Ramkumar, J., Balic, J. (2016). A new multi-objective Jaya algorithm for optimization of modern machining processes, *Advances in Production Engineering & Management,* Vol. 11, No. 4, 271-286, doi: 10.14743/apem2016.4.226.
[15] Rao, R.V. (2016). Jaya: A simple and new optimization algorithm for solving constrained and unconstrained optimization problems, *International Journal of Industrial Engineering Computations,* Vol. 7, 19-34, doi: 10.5267/j.ijiec.2015.8.004.